Cancer Research

Cathepsin B Is Dispensable for Cellular Processing of Cathepsin B-Cleavable Antibody–Drug Conjugates

Niña G. Caculitan[1], Josefa dela Cruz Chuh[1], Yong Ma[1], Donglu Zhang[1], Katherine R. Kozak[1], Yichin Liu[1], Thomas H. Pillow[1], Jack Sadowsky[1], Tommy K. Cheung[1], Qui Phung[1], Benjamin Haley[1], Byoung-Chul Lee[2], Robert W. Akita[1], Mark X. Sliwkowski[1], and Andrew G. Polson[1]

Abstract

Antibody–drug conjugates (ADC) are designed to selectively bind to tumor antigens via the antibody and release their cytotoxic payload upon internalization. Controllable payload release through judicious design of the linker has been an early technological milestone. Here, we examine the effect of the protease-cleavable valine-citrulline [VC(S)] linker on ADC efficacy. The VC(S) linker was designed to be cleaved by cathepsin B, a lysosomal cysteine protease. Surprisingly, suppression of cathepsin B expression via CRISPR-Cas9 gene deletion or shRNA knockdown had no effect on the efficacy of ADCs with VC(S) linkers armed with a monomethyl auristatin E (MMAE) payload. Mass spectrometry studies of payload release suggested that other cysteine cathepsins can cleave the VC(S) linker. Also, ADCs with a nonprotease-cleavable enantiomer, the VC(R) isomer, mediated effective cell killing with a cysteine-VC(R)-MMAE catabolite generated by lysosomal catabolism. Based on these observations, we altered the payload to a pyrrolo[2,1-c][1,4]benzodiazepine dimer (PBD) conjugate that requires linker cleavage in order to bind its DNA target. Unlike the VC-MMAE ADCs, the VC(S)-PBD ADC is at least 20-fold more cytotoxic than the VC(R)-PBD ADC. Our findings reveal that the VC(S) linker has multiple paths to produce active catabolites and that antibody and intracellular targets are more critical to ADC efficacy. These results suggest that protease-cleavable linkers are unlikely to increase the therapeutic index of ADCs and that resistance based on linker processing is improbable. *Cancer Res; 77(24); 7027–37. ©2017 AACR.*

Introduction

Combining the specificity of an antibody with the potency of chemotherapy in antibody–drug conjugates (ADC) holds much promise for the targeted eradication of malignant cells. Critical to the high therapeutic index envisioned for ADCs is the design of the linker between the antibody and the payload. Because the ADC must be delivered systemically, it is imperative that the linker not be degraded prematurely before it reaches the cancer milieu. Upon cellular internalization of the antigen-bound ADC, payload release is mediated by lysosomal processing. Several types of linkers exist: glutathione reducible, disulfide reducible, protease cleavable, acid cleavable, and noncleavable linkers (1). Out of more than 90 ADCs that entered clinical trials, only four are marketed products—ado-trastuzumab emtansine (T-DM1), inotuzumab ozogamicin, gemtuzumab ozogamicin (Mylotarg), and brentuximab vedotin (2–5). T-DM1 possesses a noncleavable linker, inotuzumab ozogamicin and Mylotarg have an acid hydrolyzable linker, and brentuximab vedotin contains the protease-cleavable dipeptide valine-citrulline (VC) linker. During early development of ADCs, protease cleavable linkers were predicted to confer exceptional control over payload release upon exposure to the corresponding proteases (6). Accordingly, the VC linker was designed to be cleaved by the cysteine protease cathepsin B (4, 7). Indeed, at least 20% of ADCs that reached clinical development use the VC linker coupled to the microtubule inhibitor, monomethyl auristatin E (MMAE) payload (1).

The rationale for the construction of a cathepsin B cleavable linker rests on several distinct characteristics. Cathepsin B belongs to a family of papain-like proteases, the cysteine cathepsins, located in the lysosome. Of the 11 family members, cathepsin B was found to be the most dominant and the most highly expressed (8). Preceding the invention of the VC linker, several studies showed that cathepsin B is upregulated in cancers, especially in metastatic tumors (8). Dubowchik and colleagues expected that the rare presence of cathepsin B in the extracellular space imparts stability on the VC linker in circulation (7). However, early work has shown that cathepsin B can be secreted, likely before cells metastasize into normal tissue (9). Cathepsin B function is also well conserved among various species (10), facilitating *in vivo* preclinical studies of VC linker-based ADCs.

[1]Genentech, Inc., South San Francisco, California. [2]23andMe, South San Francisco, California.

Note: Supplementary data for this article are available at Cancer Research Online (http://cancerres.aacrjournals.org/).

Current address of Yong Ma: Calithera Biosciences, South San Francisco, California.

Corresponding Author: Andrew G. Polson, Genentech Inc., 1 DNA Way, South San Francisco, CA 94080. Phone: 650-225-5134 ; Fax: 650-225-6240; E-mail: polson@gene.com

doi: 10.1158/0008-5472.CAN-17-2391

Despite the widespread use of protease-specific peptide cleavage (11), little is known about the determinants of the efficacy of VC-based ADCs. Here, we report an analysis of VC linker-based ADCs. We found that removal of cathepsin B did not affect the activity of ADCs and that proteases other than cathepsin B can also cleave the VC linker with varying degrees of efficiency. In addition, we show that alternative mechanisms could account for ADC efficacy independent of linker cleavage by proteases. Our data can help inform the design of ADCs and have implications about the possible mechanisms of ADC resistance.

Materials and Methods

Cell lines and reagents

The Genentech cell line repository provided the parental cancer cell lines BT-474M1, SK-BR-3, BJAB, KPL-4, and WSU-DLCL2 as well as an optimized variant of HEK293 cells, GNE 293T for lentiviral production. The BT-474M1 cell line was originally derived by subculturing BT-474 tumors grown *in vivo*. KPL-4 cells were originally obtained from Dr. J. Kurebayashi (12). Cell lines were tested with MycoAlert mycoplasma detection kit immediately before lentiviral infections and for a few months thereafter. Thawed cells are kept in use for 1 to 2 months and then a new frozen vial is used. BT-474M1, SK-BR-3, and KPL-4 express ~1 million HER2 on the membrane. BJAB cells express 6,000 and WSU-DLCL2 cells express 3,500 CD22 on the surface. BT474M-1, SK-BR-3, and KPL-4 cells were maintained in Ham's F-12:high glucose DMEM (50:50) while BJAB and WSU-DLCL2 cells were maintained in RPMI 1640. All media were supplemented with 10% heat-inactivated (or TET free, for cells with shRNA) fetal bovine serum (FBS) and 2 mmol/L L-glutamine (all from Invitrogen Corp). Stable cell lines with genetic knockout or knockdown of CTSB were generated via lentiviral infection with viral supernatant produced in GNE 293T cells according to established protocol (13). A panel of 8 gRNAs (guide RNAs that direct the targeting of the Cas9 endonuclease for genetic editing) or 6 shRNA sequences was tested (Supplementary methods). Infection with some plasmids led to nonviable cells. All cas9 cell lines were maintained in antibiotics at all times, and shRNA knockdown of CTSB was induced 3 days prior to experiments with the addition of 0.5 μg/mL doxycycline. All cell culture flasks and culture plates are tissue culture treated.

Trastuzumab (anti-HER2), 10F4v3 antibody (anti-CD22), MMAE, maleimidocaproyl para-aminobenzyl carbamate MMAE (MC-PAB-MMAE), maleimidocaproyl valine (S) citrulline para-aminobenzyl carbamate MMAE [MC-VC(S)-PAB-MMAE], maleimidocaproyl valine (R) citrulline para-aminobenzyl carbamate MMAE [MC-VC(R)-PAB-MMAE], and maleimidocaproyl valine (S) citrulline para-aminobenzyl carbamate PBD [MC-VC(S)-PAB-PBD] were prepared at Genentech. Antibody conjugates were prepared as described previously (14, 15). Thiomab site-specific conjugation technology was used for all ADCs (16). The cysteine conjugates of mAb-MC-VC(S or R)-PAB-MMAE were prepared by incubating 0.1 mmol/L MC-VC (S or R)-PAB-MMAE with 5 mmol/L cysteine for 1 hour at 37°C, and the resulting products were used to prepare the standards. Mass spectrometry (MS) characterization of two cysteine conjugates was performed in terms of retention time, accurate mass, and possible fragmentation patterns. The antibody nomenclature follows as anti-(HER2 or CD22)-VC(S or R)-payload (MMAE or PBD), with MC and PAB removed for simplicity.

Synthesis of mAb-VC(R)-PBD

The mechanistic scheme for the synthesis of the linker-payload MC-VC(R)-PAB-PBD is shown on Fig. 1. To a solution of triphosgene (140.3 mg, 0.473 mmol) in dry dichloromethane (DCM; 5.0 mL) was added a solution of compound **1** (1.0 g, 1.05 mmol) and Et_3N (265.2 mg, 2.6 mmol) in dry DCM (15.0 mL) dropwise in ice bath. It was stirred at 27°C for 1.0 hours under N_2. Then a solution of compound **2** (601.4 mg, 1.10 mmol) and Et_3N (265.2 mg, 2.6 mmol) in DMSO (8.0 mL) was added to the freshly prepared isocyanate. The mixture was stirred at 27°C for 2.0 hours. The mixture was diluted with H_2O (30.0 mL), extracted with DCM (60.0 mL × 3). The organic layer was washed with brine (30.0 mL) and H_2O (30.0 mL), dried over Na_2SO_4, concentrated, and purified by flash column chromatography (DCM: Methanol = 10:1) to give the product as a yellow solid (220.0 mg, 13.8%).

A mixture of HOAc/H_2O (3/1, 8.0 mL) was added to a solution of compound **3** (180 mg, 0.116 mmol) in tetrahydrofuran (THF; 3.0 mL) and the mixture was stirred at 27°C for 18.0 hours. The pH of the reaction mixture was adjusted to 8.0 with a saturated $NaHCO_3$ solution (50.0 mL). The mixture was extracted with EtOAc (60.0 mL × 3) and the combined extracts were washed with saturated $NaHCO_3$ solution (60.0 mL), water (60.0 mL), brine (60.0 mL), dried over Na_2SO_4, and concentrated. It was purified by flash column chromatography (DCM:MeOH = 10:1) to give the product as a yellow solid (120.0 mg, 77.9%).

To a solution of compound **4** (120 mg, 0.100 mmol) in DMSO (4.5 mL) was added 2-iodobenzoic acid (IBX; 76.2 mg, 0.30 mmol). The mixture was stirred at 20°C for 48.0 hours. It was purified by prep-HPLC (FA system) to give the product as a white solid (30 mg, 25.2%).

Trifluoroacetic acid (TFA; 2.0 mL) was added dropwise to compound **5** (30.0 mg, 22.7 μmol) at 0°C and the mixture was stirred at 0°C for 20 minutes. The mixture was added to a saturated $NaHCO_3$ solution (50.0 mL) dropwise at 0°C and it was extracted with DCM (30.0 mL × 3). The organic layer was dried over Na_2SO_4 and concentrated to give the desired product as a yellow solid (14.9 mg, 53.8%). LCMS (10–80, AB, 7.0 minutes): RT = 1.044 minutes, $[M/2+1]^+$ 601.4.

Cell viability assays

Tumor cell viability in the presence of the ADCs was measured using Cell Titer-Glo (Promega Corp.). Cells were plated in black-walled 96-well plates at densities in accordance with their doubling time. They were then incubated overnight at 37°C in a humidified atmosphere of 5% CO_2 prior to ADC addition. For adherent BT474M-1 and KPL-4 cells, cell media were aspirated and replaced with fresh media containing dose titrations of anti-HER2 ADCs. For lymphoma cell lines BJAB and WSU-DLCL2, fresh media containing dose titrations of anti-CD22 ADCs at 5-fold potency at the appropriate volume for final 1-fold potency were added. Cells were incubated with the ADCs for various time points as indicated. All conditions were done in triplicates and experiments performed at least thrice. Cellular ATP levels (an indicator of cell count) were determined by addition of Cell Titer-Glo reagent, 10 minutes

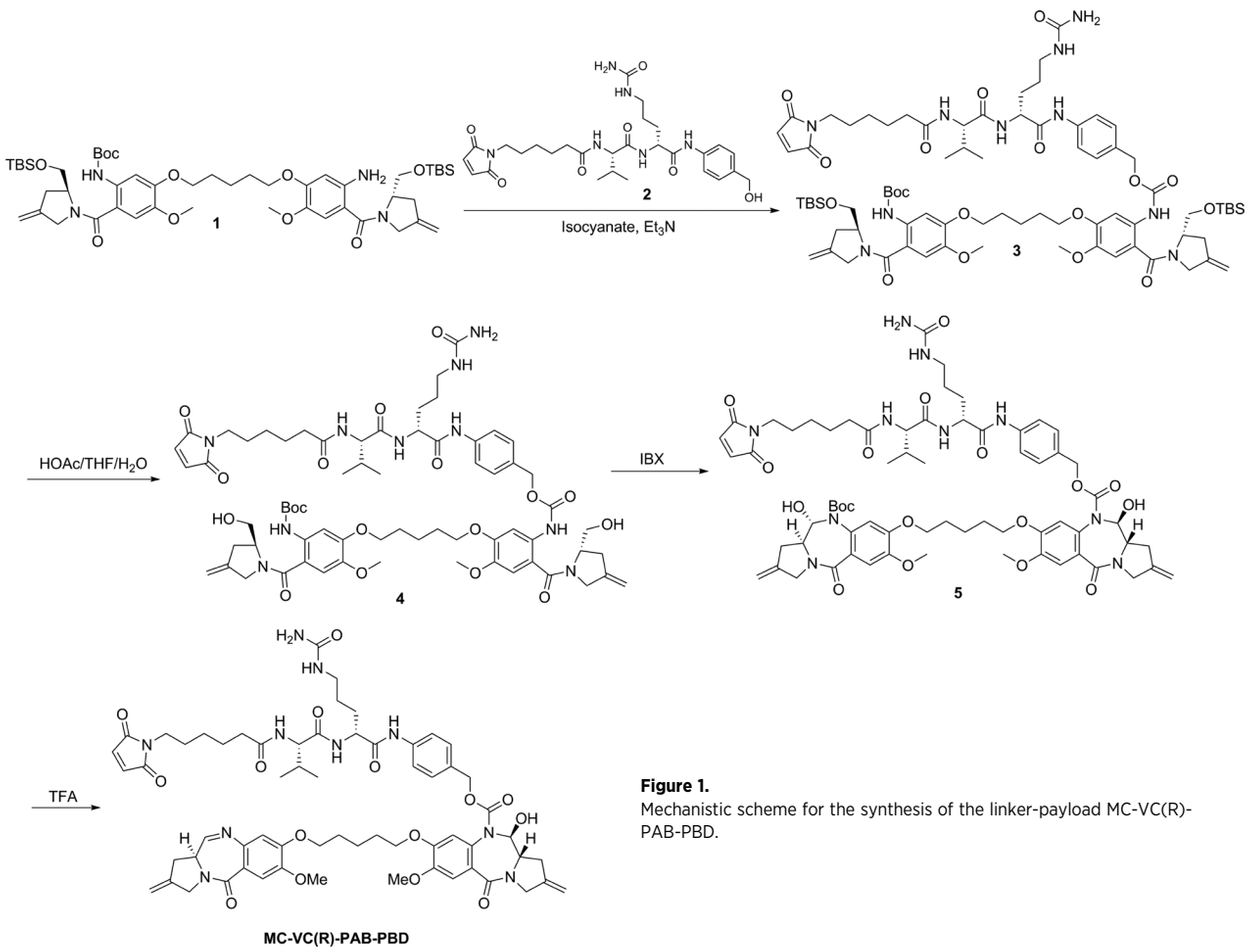

Figure 1.
Mechanistic scheme for the synthesis of the linker-payload MC-VC(R)-PAB-PBD.

incubation at room temperature, and the luminescent signal was measured with a Packard/Perkin-Elmer TopCount. For all cellular assays, dose–response curves were generated using Prism 7 software (GraphPad).

Quantitation of free MMAE release from ADCs internalized by cells

Cells were plated as before in 96-well flat (adherent cells) or round (suspension cells) bottom plates 24 hours prior to ADC addition. ECHO acoustic liquid handling technology (Labcyte Inc.) was used to add an ADC dose titration of 0 to 10 μg/mL in duplicate. After 2 and 24 hours of ADC incubation at 37°C and 5% CO_2, plates were spun down to enable separate processing of the cells and the supernatant. Proteins in the cell lysate or the supernatant were precipitated with acetonitrile, and lyophilized pellets were produced from the resulting supernatants. The lyophilized pellets were reconstituted in 120 μL of water (Optima LC/MS, Fisher Chemical). 10 μL of sample was injected to an AB SCIEX QTRAP 6500 mass spectrometer coupled with Waters liquid chromatography. Free MMAE standard curves (10 points) were prepared for quantitation using untreated cell lysates. Additional details are in the supplementary methods.

Quantitation of free MMAE release from ADCs exposed to purified proteases with liquid chromatography-mass spectrometry/mass spectrometry

The ability of cysteine cathepsins B, K, L, S, and human liver lysosomal extract to cleave the VC(S) linker was assessed by liquid chromatography-mass spectrometry (LC-MS), MRM-based quantitation method. The loss of the linker-payload moiety from the anti-HER2-VC(S)-MMAE ADC and relative amounts of free MMAE produced were measured concurrently. 1 μmol/L of the ADC is incubated for 4 hours at 37°C with either 20 nmol/L of the cysteine cathepsin or 0.2 mg/mL of human liver lysosomal extract in the presence of 0.04 mmol/L dithiothreitol and 10 mmol/L 2-morpholin-4-ylethanesulfonic acid (MES) buffer pH 6. The reactions are quenched with an equal volume of 2% formic acid. Each experiment was performed in triplicate, and a total of three separate experiments were conducted. For the LC-MS/MS measurements, 10 μL ADC samples were injected and loaded onto a Waters C4 column (1.7 μm, 300 Å pore size, 0.3 × 50 mm) maintained at 65°C. Please refer to the supplementary methods for specific details on the protocol and analysis.

Catabolite identification by LC-MS/MS

KPL-4 cells were plated in T75 culture flasks and, after 24 hours, were incubated with anti-HER2-VC(S)-MMAE and anti-HER2-VC

(R)-MMAE ADCs for 1 hour at 37°C. The media were then replaced with fresh media and cells were incubated at 37°C for another 3 or 23 hours for a total of 4 or 24 hour incubation. Drugs were added to the cell media and then removed within minutes of exposure for the 0-hour control. All conditions were done in triplicates. In the trypsinized cells, all media and PBS washes after supernatant collection were separately collected and analyzed. The collected PBS and culture supernatant samples were concentrated by solid-phase extraction (SPE) before analysis. An aliquot of 400 μL supernatant from each sample was applied to a preconditioned C18 SPE column. The SPE column was washed with 1 mL water before eluted with 600 μL methanol:acetonitrile 1:1 (v/v) containing 10 nmol/L MMAE-d8 as the internal standard (IS). The eluate was evaporated to ~200 μL under N_2 gas flow. The standard curve samples were prepared similarly in fresh cell culture media.

Cell pellets were suspended in 1 mL water. An aliquot of 400 μL cell suspension was extracted with 400 μL methanol: acetonitrile 1:1 (v/v) containing 10 nmol/L MMAE-d8 as the IS. The solution was centrifuged, transferred to a new tube, and evaporated to ~100 μL under N_2 gas flow. 100 μL of methanol was added to each sample before injection onto LC-MS. The standard curve samples were prepared similarly with a suspension of untreated cells. The LC-MS/MS analysis was conducted on a Shimadzu Nexera HPLC system coupled to a Sciex Qtrap 6500 mass spectrometer with an IonDrive Turbo V source (Sciex) in the positive ion mode. Please refer to the supplementary methods for specific details of column conditions, data collection, and analysis.

Results

Loss of cathepsin B has no effect on the VC(S)-MMAE ADC efficacy

The VC linker was designed to be cleaved by cathepsin B upon ADC trafficking to the lysosome (7). However, although it has been shown that purified cathepsin B can effectively cleave the VC linker, whether it is strictly required for intracellular linker cleavage has not been demonstrated. We examined the extent to which cathepsin B-specific cleavage is important in mediating cell killing by VC-MMAE ADCs. We performed CRISPR gene deletion of CTSB in HER2-overexpressing cell lines (KPL-4 and BT-474M1) and doxycycline-inducible expression of an shRNA against cathepsin B in $CD22^+$ lymphoma lines (WSU-DLCL2 and BJAB). The gRNA and shRNA that led to the largest loss in CTSB expression were used for experiments. The enzymatic activity of cathepsin B was reduced to less than 5% of the activity in the parental cell lines based on a fluorogenic assay (Supplementary Fig. S1). The mRNA and protein expression data also confirm the loss of cathepsin B (Supplementary Fig. S1).

In spite of the greatly reduced levels of cathepsin B in these knockout/knockdown cell lines, no consequent change in ADC efficacy was observed. Dose titrations of the anti-HER2 or anti-CD22 VC-MMAE ADCs (Fig. 2A) were added to the respective parental cells and cathepsin B deficient cells for viability assays (Fig. 2B and C, and Supplementary Fig. S2A and S2B). No significant difference was observed for the IC_{50} values of KPL-4 parental cells (0.028 μg/mL) and cathepsin B deletion cells (0.034 μg/mL) or WSU-DLCL2 parental cells and cathepsin B knockdown cells (IC_{50} = 0.071 μg/mL for both). Similar experiments performed using the small molecule CA074ME, a cell-permeable inhibitor against cathepsin B, were consistent with these findings (Supplementary Fig. S3A–S3C).

To understand why loss of cathepsin B had no apparent effect on the cytotoxicity of the VC-MMAE ADCs, we investigated the effect of cathepsin B on ADC processing. Specifically, we directly quantified the contribution of cathepsin B to the cleavage of the VC linker. Mass spectrometry was used to measure the cellular concentration of the cleavage product, free MMAE (Fig. 2D), after parental or cathepsin B deficient cells were exposed to the ADCs for 24 hours. No statistically significant decrease in the free MMAE product was observed in the absence of cathepsin B in KPL-4 or WSU-DLCL2 cells (Fig. 2E and F). The cellular concentration of free MMAE in KPL-4 cells is at least 20-fold greater than that in WSU-DLCL2 cells at similar ADC concentrations. The much higher copy number of HER2 on the KPL-4 cell surface (~1×10^6 copies) than CD22 on WSU-DLCL2 cells (~4×10^3 copies), as well as differential intracellular trafficking, may account for this difference (15, 17).

Other cysteine cathepsins can cleave the VC(S) linker

The expression profiles of different cathepsin proteases can vary from cell type to cell type, thereby affecting the overall proteolytic activity within a given cell (Supplementary Fig. S4). Within each cell, redundancies in enzymatic function of cysteine cathepsins and overlap in substrate specificities may allow other cysteine cathepsins to compensate for the loss of cathepsin B. We explored whether other cysteine cathepsins could process the VC(S) linker by using mass spectrometry to measure the cleavage products upon exposure of the ADCs to purified cathepsins (B, K, L, and S), and human liver lysosomal extract containing a mixture of proteases. The anti-HER2-VC(S)-MMAE ADC (1×10^{-4} μg/mL) was incubated with 20 nmol/L of the purified proteases or 0.2 mg/mL of the human liver lysosomal extract for 3 hours at 37°C. Quantitative LC-MS allows for detection of the intact antibody, antibody that has released the free MMAE payload, and the free MMAE product itself. The drug-to-antibody ratio (DAR) for the anti-HER2-VC(S)-MMAE ADC used in these experiments was 2.

The mass spectrum of the untreated control sample contains a single peak at 147,888 m/z that corresponds to the intact ADC (Supplementary Fig. S5). Samples that were incubated with proteases exhibited ADC processing to varying degrees (Fig. 3A–E). ADC exposed to cathepsin B resulted in loss of both MMAE moieties (146,189 m/z) with no detectable amount of other cleavage products. Intermediate processing is evident upon exposure to cathepsins K and L, with peaks at 147,892, 146,192, and 147,043. The last peak denotes the loss of one MMAE moiety. Human liver lysosomal extract has a dominant peak at 146,221 m/z that roughly corresponds to the fully cleaved ADC. However, the heterogeneity of the enzymatic mixture in the lysosomal extract makes it difficult to predict the exact modifications that occurred. Results are tabulated in Table 1.

Mass spectrometry results for antibody processing correlated well with the quantitation of free MMAE payload released (Fig. 3F). Negligible amount of free MMAE was measured in the control, followed by intermediate levels of free MMAE with cathepsins K and L, and high levels of the payload for the lysosomal extract and cathepsins B and S. Thus, although the VC

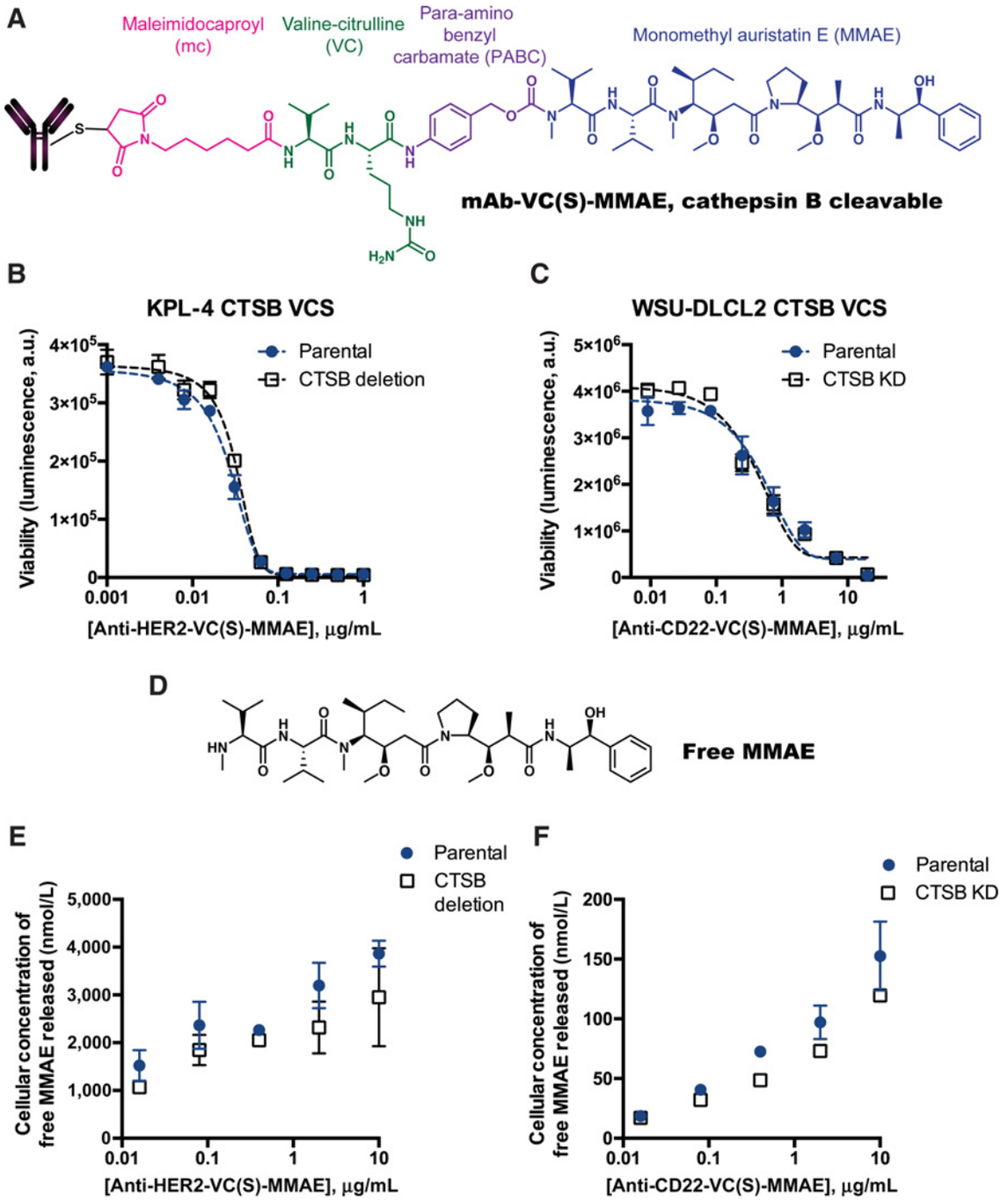

Figure 2.

A, Structure of mAb-VC(S)-MMAE. Proliferation assays for anti-HER2-VC(S)-MMAE in KPL-4 parental and CTSB deletion cells (**A**) and anti-CD22-VC(S)-MMAE in WSU-DLCL2 parental and CTSB knockdown cells (**B**). **D,** Structure of the predicted free MMAE product released from the ADC upon proteolytic processing. Cellular concentrations of free MMAE measured via mass spectrometry in parental or CTSB-deficient cells exposed to their respective ADCs, KPL-4 cells with anti-HER2-VC(S)-MMAE (**E**), and WSU-DLCL2 cells with anti-CD22-VC(S)-MMAE (**F**).

linker should be cleaved specifically by cathepsin B, these mass spectrometry measurements demonstrated that there are redundancies in the cleavage of the VC linker by other cysteine cathepsins.

Cysteine-VC-MMAE catabolite, like free MMAE, can induce cell killing

The VC-MMAE moiety is tethered to the antibody via conjugation of the thiol group on the antibody with maleimidocaproyl,

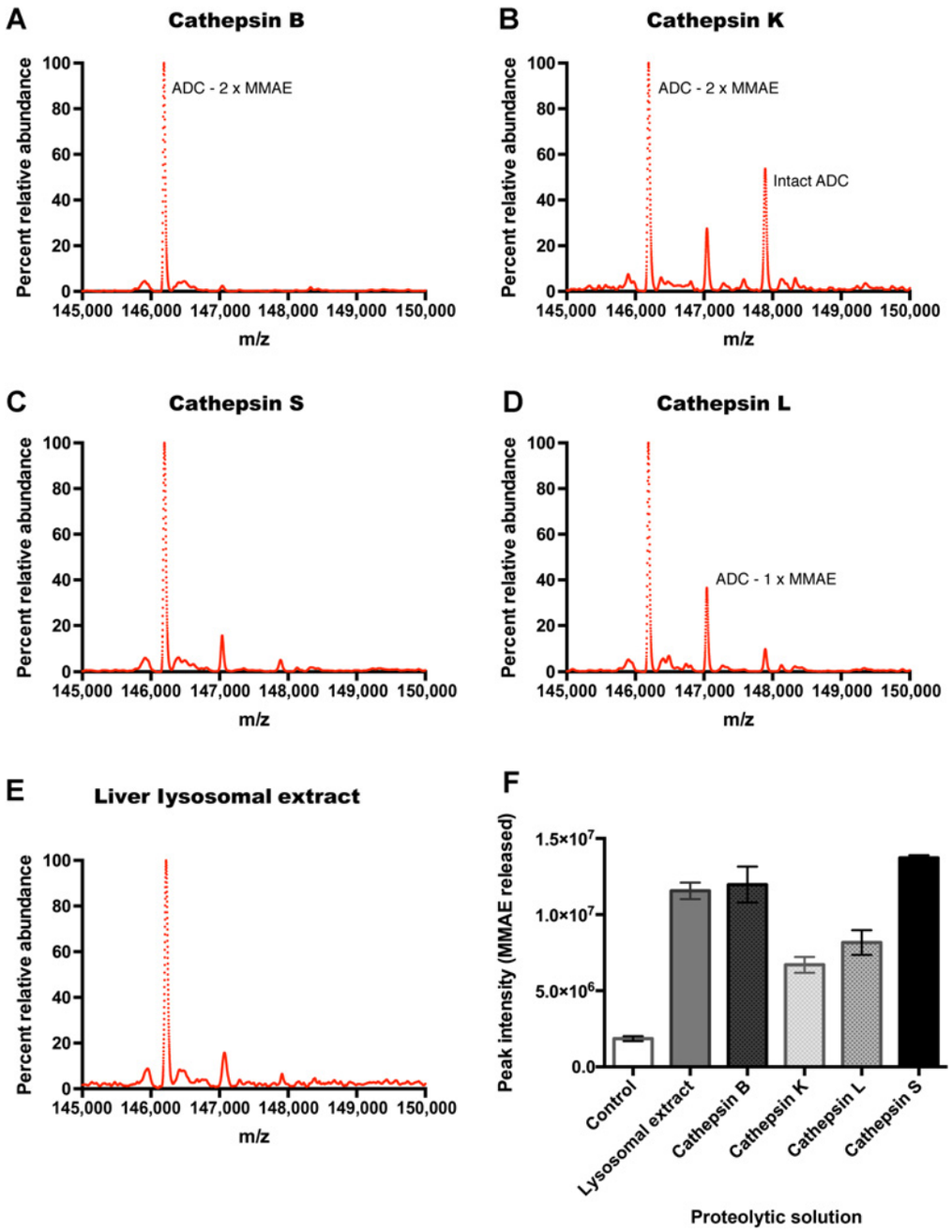

Figure 3.

Spectra obtained via quantitative LC-MS/MS for the anti-HER2-VC(S)-MMAE after 3-hour exposure to different proteolytic solutions: cathepsin B (**A**); cathepsin K (**B**); cathepsin S (**C**); cathepsin L (**D**); and liver lysosomal extract (**E**). **F,** Quantitation of free MMAE released upon exposure of the anti-Her2-VC(S)-MMAE to various proteolytic solutions.

as shown in Fig. 1A. Previous reports have shown that ADCs wherein MMAF (an analog of MMAE) is directly conjugated to MC without the cleavable VC linker can still be cytotoxic (18). We wondered whether a similar catabolite might exist independent of protease cleavage of the VC-MMAE ADCs. We studied this by taking advantage of the stereoselectivity of the cysteine cathepsins. ADCs that possess the VC(R) isomer, a stereoisomer of the VC(S) linker, were used (Fig. 4A). This linker should be resistant to protease cleavage, preventing the release of free MMAE and thereby impairing ADC cytotoxicity. The anti-HER2-VC(R)-MMAE is still effective in inducing cell death as shown by cell viability assays for the KPL-4 parental line (IC_{50} = 0.063 μg/mL) and cells with the cathepsin B deletion (IC_{50} = 0.085 μg/mL; Fig. 4B). The VC(R)-MMAE ADC is approximately

Table 1. Percent relative abundance of the intact anti-HER2-VC(S)-MMAE ADC and various products after loss of the MMAE molecules upon exposure to different proteolytic solutions

	Percent of each species		
Sample	**Intact ADC**	**ADC-1 × MMAE**	**ADC-2 × MMAE**
Control	100	0	0
Cathepsin B	0	0	100
Cathepsin K	29.64	15.18	55.18
Cathepsin L	0	26.75	73.25
Cathepsin S	0	0	100
Lysosomal extract	0	0	100

half as potent as the VC(S)-MMAE ADC. As expected, quantitation of the free MMAE release via mass spectrometry reveals that no free MMAE product is released by the cells exposed to the VC(R)-MMAE ADC, regardless of cathepsin B expression (Fig. 4C).

We set out to identify the active catabolite that might play a role in the efficacy of ADCs with the noncleavable VC(R) isomer. Based on the predicted pathway of processing for VC-MMAE ADCs (Supplementary Fig. S6), the catabolite cys-VC(R)-MMAE should be produced after the initial lysosomal catabolism. Using mass spectrometry, we measure the concentration of the cys-VC-MMAE product at 0, 4, and 24 hours after addition of the anti-HER2-VC-MMAE ADCs [VC(S) or VC(R) isomer] in the cell lysate and media of parental or cathepsin B deleted cells. The amount of the two catabolites in cells that were exposed to the ADCs for only a few minutes is negligible and measured values are below the threshold for accurate measurement. This was taken to be the baseline at time 0. For the 4 and 24 hour timepoints, parental and cathepsin B deficient cells exposed to VC(S)-MMAE ADC showed high levels of the free MMAE product while cells exposed to the VC(R)-MMAE ADC had levels similar to the control (Fig. 4D). Conversely, the cys-VC-MMAE catabolite was present at high levels in the VC (R)-MMAE ADC exposed cells but not in the VC(S)-MMAE ADC exposed cells (Fig. 4E). The attenuated, but still potent, cytotoxicity of the ADC with the VC(R) linker points to the robustness of cellular processing of the ADC. Moreover, our results suggest that multiple mechanisms exist in the production of effective catabolites. The inhibitory capacity of these catabolites against the intracellular target, such as microtubules in this case, helps determine ADC efficacy.

Cytotoxicity of the pyrrolobenzodiazepine payload is sensitive to linker cleavage

Given the importance of target–catabolite interaction in ADC potency, we next tested whether a cleavage-dependent payload would sensitize the VC-based ADCs to loss of cathepsin B and protease cleavage in general. The PBD dimer, an alkylating and cross-linking agent that binds to the minor groove of DNA, is now a widely used payload for ADCs (19–22). The most developed of these is rovalpituzumab tesirine, which is currently in Phase 2 and Phase 3 clinical trials (21, 23). PBD dimers with dipeptide cleavable linkers attached to the N10 nitrogen of the PDB dimer, like rovalpituzumab tesirine, may not be active unless the linker is fully released, as the C10-N10 imine double bond is one of the active alkylating groups. Additionally, traceless release of the free drug has been shown to be required before the payload can fit in the minor groove of DNA (24).

Anti-HER2-VC-PBD ADCs with either the cleavable or the noncleavable isomer of the VC linker (Fig. 5A and B) were prepared and tested in cell viability assays with both parental and CTSB knockout cell lines (Fig. 5C–F). Loss of cathepsin B in KPL-4 cells does not affect their response to anti-HER2-VC(S)-PBD, with IC_{50} values of 0.15 μg/mL and 0.11 μg/mL for the parental and cathepsin B deletion cells, respectively. For BT-474M1 cells, we observe minimal difference in response between parental cells (IC_{50} = 0.022 μg/mL) and cathepsin B deletion cells (IC_{50} = 0.055 μg/mL) to the VC(S)-PBD ADC. In contrast, KPL-4 cells, regardless of cathepsin B status, are unresponsive to the VC(R)-PBD isomer. BT-474M1 cells are more responsive, but still display at least 20-fold decrease in sensitivity to the VC(R) isomer versus the VC(S) isomer against the parental cells (IC_{50} = 0.83 μg/mL) and cathepsin B deletion cells (IC_{50} = 1.3 μg/mL). Overall viability is also affected, with 10% of the parental BT-474M1 cells and 40% of the cathepsin B deletion cells still viable at 10 μg/mL of the anti-HER2-VC(R)-PBD. The difference in the IC_{50} values between the parental BT-474M1 cells and the CTSB knockout cells is negligible. BJAB parental and cathepsin B knockdown cells also displayed the large differential in response to the anti-CD22-VC(S)-PBD versus the anti-CD22-VC(R)-PBD ADC (Supplementary Fig. S7).

Discussion

Although the VC linker was designed to be cleaved specifically by cathepsin B, loss of cathepsin B had no effect on the efficacy of VC-based ADCs. Cytotoxicity by VC(S)-MMAE ADCs against two different targets, HER2 and CD22, in HER2 overexpressing cells and lymphoma lines, respectively, was unabated by the loss of cathepsin B function. Other cysteine cathepsins were suspected to play a role, but this is the first study to systematically investigate the importance of cathepsin B-specific cleavage by genetic loss. We found similar results with the cathepsin B inhibitor CA074ME, but one must be careful with the dose level of pharmacological inhibitors in such studies. High doses as well as the cell permeable methyl ester form of CA074 can inhibit cysteine cathepsins nonspecifically (25).

We found that other cysteine cathepsins can compensate for the loss of cathepsin B. Cysteine cathepsins tested (B, K, L, and S) and human liver lysosomal extracts cleaved the ADC with varying degrees of efficiency. Both cathepsins B and S had similar levels of efficacy while cleavage of the VC linker by cathepsins K and L was not as efficient. Previous work mapping the amino acid preferences at specific positions on the substrates revealed that cathepsin L and cathepsin B substrate specificities can diverge considerably (26). We observed that the distribution of the cathepsins can vary depending on cell type (Supplementary Fig. S4 and Supplementary Methods). Concomitantly, the degree of compensation by the different cathepsins for the cleavage of the VC linker can also vary. For example, we found that immune

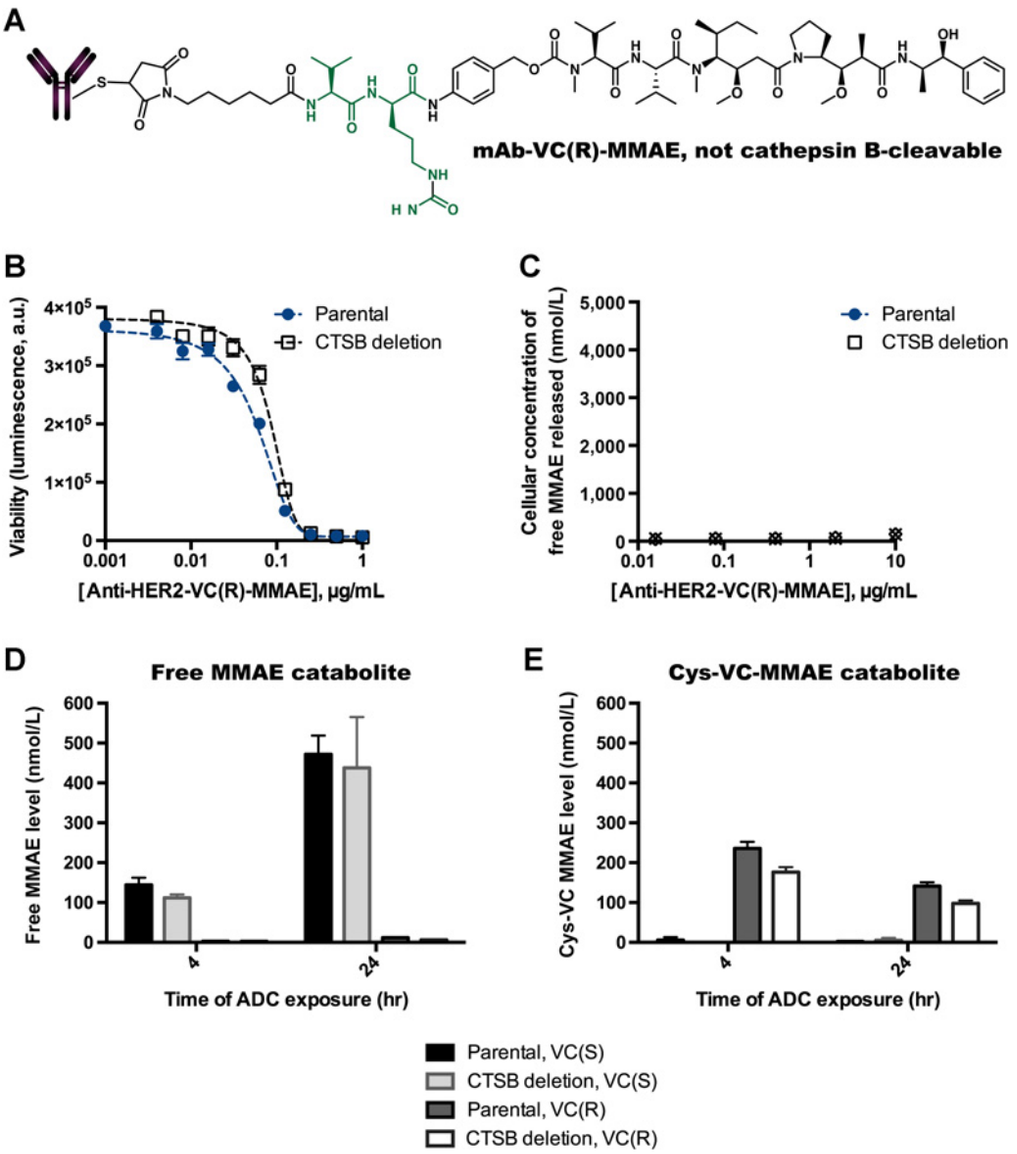

Figure 4.

A, Structure of the anti-HER2-VC(R)-MMAE ADC. **B** and **C**, Proliferation assay (**B**) and quantitation of cellular concentration of the free MMAE via LC-MS/MS (**C**) for KPL-4 parental and CTSB deletion cells in the presence of anti-HER2-VC(R)-MMAE ADC. LC-MS/MS quantitation of the free MMAE catabolite (**D**) and Cys-VC-MMAE catabolite (**E**) for KPL-4 parental and CTSB deletion cells after exposure to the VC(S) or VC(R) isomer of the anti-HER2-VC-MMAE ADC.

cells (RAW 264.7 and Toledo) contained a greater variety of cathepsins and the relative quantities of these proteases were closer in value than in HER2 overexpressing cell lines (Founder5, SK-BR3, and BT-474). The overlapping catalytic activities of the cysteine cathepsins for VC-MMAE ADCs were consistent with findings for other conjugates and hydrolytic enzymes. Other cysteine cathepsins, such as cathepsins L, S, and Z, can compensate for the loss of cathepsin B in the growth of tumors (27–29). Dubowchik and colleagues posited that other enzymes in liver extracts might contribute to the faster digestion rate observed with lysosomal extracts versus purified cathepsin B (7).

Cleavage of the VC(S) linker is not unique to lysosomal cysteine cathepsins. Dorywalska and colleagues demonstrated that carboxylesterase 1c present in rodent serum could also cleave the VC linker, leading to increased toxicities of the ADCs in rodents (30). A noninternalizing ADC, coupled with various protease cleavable linkers, including the VC(S) linker, was also recently shown to still inhibit tumor growth in mouse xenografts (31). Aside from carboxylesterase 1c, extracellular cleavage may be carried out by secreted cathepsins and other degradative proteases in the tumor microenvironment (32–34). Previous work coupled with the data we report here point to multiple cleavage possibilities that can lead to payload release

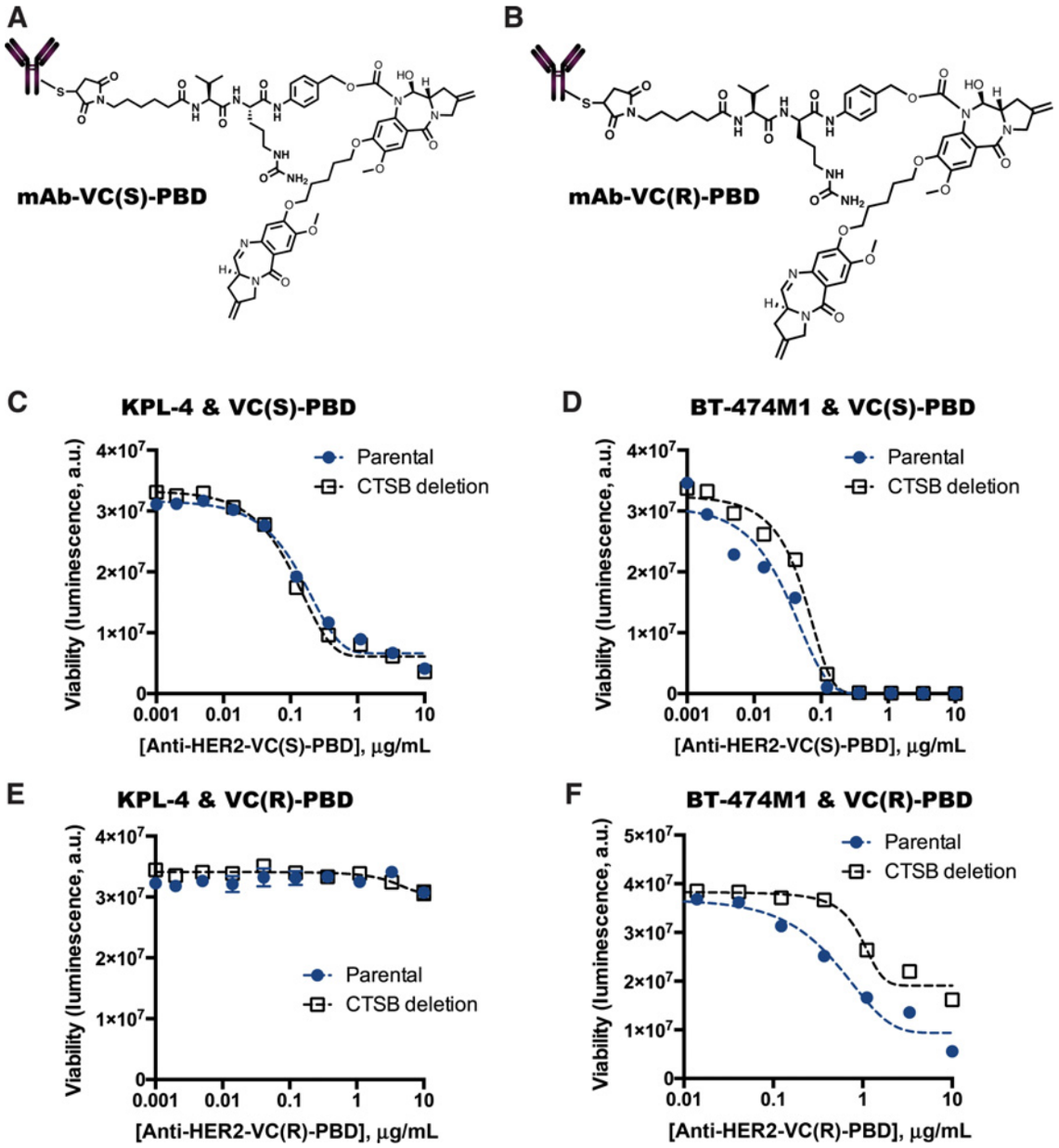

Figure 5.

Structures of the VC(S) isomer (**A**) and VC(R) isomer (**B**) of the anti-HER2-VC-PBD ADC. Proliferation assays for KPL-4 (**C–E**) and BT-474M1 (**D–F**) parental and cathepsin B deletion cells after exposure to anti-HER2-VC(S)-PBD (**C** and **D**) and anti-HER2-VC(R)-PBD (**E** and **F**) ADCs.

by protease-specific cleavable linkers. Thus, ADC processing is not as controllable as intended.

Analysis of the catabolites of the noncleavable anti-HER2-VC(R)-MMAE ADC reveals that cleavage of the VC linker is not even necessary to mediate ADC cytotoxicity. The major catabolite for this ADC was identified to be cys-VC-MMAE. In the absence of free MMAE, cys-VC-MMAE induced cell killing. However, the IC_{50} for VC(R)-MMAE ADC is 2–3-fold higher than for the cathepsin B cleavable VC(S)-MMAE ADC. Cys-VC-MMAE is the first product of simple lysosomal catabolism, the first step of ADC processing. It must still be able to bind to the microtubules and induce cell killing in its uncleaved form. Doronina and colleagues have found that MC-MMAF can produce a cysteine adduct that is cytotoxic (18). For T-DM1, which possesses an uncleavable SMCC linker, complete proteolytic degradation of the anti-HER2 antibody can release the lysine-*N*ε-MCC-DM1 catabolite. Like the parental maytansine, this catabolite also binds to microtubules, inducing cell death (35, 36). Interestingly, we found that anti-HER2-MC-MMAE is roughly 10-fold less cytotoxic than

anti-HER2-VC(S)-MMAE and about 3-fold less cytotoxic than anti-HER2-VC(R)-MMAE (Supplementary Fig. S8). The disparity between MC-MMAE and VC(R)-MMAE ADCs may be due to the efficiency of a number of processes, such as antibody degradation, transport across the lysosomal membrane, and binding to microtubules or tubulin dimers. In any case, our results show that alternative catabolites of MMAE are still remarkably effective.

ADC efficacy can be made to be more dependent on linker cleavage when it bears a payload that is optimally active only when fully cleaved. We achieve this by replacement of the MMAE payload with a PBD payload. The specific chemistry of PBD in DNA alkylation requires that it be fully cleaved from the VC linker to achieve its optimal inhibitory effect. As predicted, the cleavable VC(S)-PBD ADC was much more effective than the noncleavable VC(R)-PBD ADC in inducing cell killing in HER2 overexpressing cells and lymphoma cells. Loss of cathepsin B in BT-474M1 cells, but not in KPL-4 cells, resulted in a mild shift in the IC_{50} value. This reiterates the existence of redundancies among cell proteases.

Quantitation of the free MMAE release suggests that the antibody target is a determinant of ADC efficacy. HER2-overexpressing cells were loaded with 20-fold more intracellular free MMAE than the lymphoma cell lines. This can be attributed to the differences in the copy number and the trafficking patterns of the HER2 and CD22 targets upon internalization. HER2 copy number per cell on the surface of over-expressing epithelial cells is three orders of magnitude greater than CD22 copy number per lymphoid cell. However, the vast majority of CD22 is rapidly trafficked to the lysosome (15) but only ~15% of HER2 is trafficked there, with the rest undergoing rapid recycling back to the plasma membrane (17). Roughly speaking, this explains why the difference in cellular free MMAE concentration is only 20-fold and not more in spite of the much greater number of HER2 that the ADCs can bind. Nevertheless, higher payload release can mean better killing potency. Thus, specific target biology should be taken into account when considering linker-payload conjugation. The resulting combinations should also be empirically tested.

Our analyses elucidate the various determinants of the cell killing potencies of ADCs. The antibody target and the payload-target interface are likely the most important factors. We find that cathepsin B expression is less relevant to the processing of ADCs than generally thought (11). Thus, the preferential expression of cathepsin B, or other specific proteases, in cancers would not necessarily increase the therapeutic index of ADCs. However, the broader possibilities for linker processing also suggest that tumors are unlikely to be less sensitive to ADCs, or become resistant to them, due to lack of expression of the proper proteases. Consistent with this, a CRISPR screen of proteases that induce resistance to VC linker-based ADCs did not yield any genes that affected linker processing (manuscript in preparation). These findings can help guide the design of future ADCs for maximal efficacy and optimal therapeutic window. Beyond ADCs, our results may also be instructive for the development of emerging therapeutics that are dependent on cleavage technologies, such as antibody–antibiotics conjugates (37, 38). Understanding how protease-cleavable linkers operate can help better design and anticipate challenges for these types of therapies.

Disclosure of Potential Conflicts of Interest

N.G. Caculitan is a postdoctoral researcher at Genentech. No potential conflicts of interest were disclosed by the other authors.

Authors' Contributions

Conception and design: N.G. Caculitan, Y. Liu, T.H. Pillow, J. Sadowsky, M.X. Sliwkowski, A.G. Polson

Development of methodology: J. dela Cruz Chuh, Y. Ma, D. Zhang, Y. Liu, J. Sadowsky, B. Haley, B.-C. Lee, M.X. Sliwkowski

Acquisition of data (provided animals, acquired and managed patients, provided facilities, etc.): N.G. Caculitan, Y. Ma, Y. Liu, T.K. Cheung, B.-C. Lee, R.W. Akita

Analysis and interpretation of data (e.g., statistical analysis, biostatistics, computational analysis): N.G. Caculitan, J. dela Cruz Chuh, Y. Ma, D. Zhang, K.R. Kozak, Y. Liu, J. Sadowsky, T.K. Cheung, M.X. Sliwkowski

Writing, review, and/or revision of the manuscript: N.G. Caculitan, J. dela Cruz Chuh, Y. Ma, K.R. Kozak, T.H. Pillow, B.-C. Lee, R.W. Akita, M.X. Sliwkowski, A.G. Polson

Administrative, technical, or material support (i.e., reporting or organizing data, constructing databases): J. dela Cruz Chuh, Q. Phung, B.-C. Lee

Study supervision: M.X. Sliwkowski

Acknowledgments

We thank Carter Fields, Jun Guo, and Ginny Li for technical advice, Peter Senter and Damon Meyer (Seattle Genetics, Inc., Bothell, WA) for the VC-MMAE technology and Gail Phillips, Paul Polakis, Hans Erickson, and Peter Dragovich for helpful discussions.

The costs of publication of this article were defrayed in part by the payment of page charges. This article must therefore be hereby marked *advertisement* in accordance with 18 U.S.C. Section 1734 solely to indicate this fact.

Received August 17, 2017; revised September 18, 2017; accepted October 13, 2017; published OnlineFirst October 18, 2017.

References

1. Jain N, Smith SW, Ghone S, Tomczuk B. Current ADC linker chemistry. Pharm Res 2015;32:3526–40.
2. LoRusso PM, Weiss D, Guardino E, Girish S, Sliwkowski MX. Trastuzumab emtansine: a unique antibody-drug conjugate in development for human epidermal growth factor receptor 2-positive cancer. Clin Cancer Res 2011;17:6437–47.
3. DiJoseph JF, Armellino DC, Boghaert ER, Khandke K, Dougher MM, Sridharan L, et al. Antibody-targeted chemotherapy with CMC-544: A CD22-targeted immunoconjugate of calicheamicin for the treatment of B-lymphoid malignancies. Blood 2004;103:1807–14.
4. Doronina SO, Toki BE, Torgov MY, Mendelsohn BA, Cerveny CG, Chace DF, et al. Development of potent monoclonal antibody auristatin conjugates for cancer therapy. Nat Biotechnol 2003;21:778–84.
5. Hamann PR, Hinman LM, Hollander I, Beyer CF, Lindh D, Holcomb R, et al. Gemtuzumab ozogamicin, a potent and selective anti-CD33 antibody-calicheamicin conjugate for treatment of acute myeloid leukemia. Bioconjugate Chem 2002;13:47–58.
6. de Groot FM, Damen EW, Scheeren HW. Anticancer prodrugs for application in monotherapy: Targeting hypoxia, tumor-associated enzymes, and receptors. Curr Med Chem 2001;8:1093–122.

7. Dubowchik GM, Firestone RA, Padilla L, Willner D, Hofstead SJ, Mosure K, et al. Cathepsin B-labile dipeptide linkers for lysosomal release of doxorubicin from internalizing immunoconjugates: Model studies of enzymatic drug release and antigen-specific in vitro anticancer activity. Bioconjugate Chem 2002;13:855–69.
8. Mohamed MM, Sloane BF. Cysteine cathepsins: multifunctional enzymes in cancer. Nat Rev Cancer 2006;6:764–75.
9. Poole AR, Tiltman KJ, Recklies AD, Stoker TA. Differences in secretion of the proteinase cathepsin B at the edges of human breast carcinomas and fibroadenomas. Nature 1978;273:545–7.
10. Otto H-H, Schirmeister T. Cysteine proteases and their inhibitors. Chem Rev 1997;97:133–72.
11. Choi KY, Swierczewska M, Lee S, Chen X. Protease-activated drug development. Theranostics 2012;2:156–78.
12. Kurebayashi J, Otsuki T, Tang CK, Kurosumi M, Yamamoto S, Tanaka K, et al. Isolation and characterization of a new human breast cancer cell line, KPL-4, expressing the Erb B family receptors and interleukin-6. Br J Cancer 1999;79:707–17.
13. Singer O, Tiscornia G, Ikawa M, Verma IM. Rapid generation of knockdown transgenic mice by silencing lentiviral vectors. Nat Protoc 2006;1:286–92.
14. Polson AG, Williams M, Gray AM, Fuji RN, Poon KA, McBride J, et al. Anti-CD22-MCC-DM1: An antibody-drug conjugate with a stable linker for the treatment of non-Hodgkin's lymphoma. Leukemia 2010;24:1566–73.
15. Polson AG, Calemine-Fenaux J, Chan P, Chang W, Christensen E, Clark S, et al. Antibody-drug conjugates for the treatment of Non-Hodgkin's Lymphoma: target and linker-drug selection. Cancer Res 2009;69:2358–64.
16. Junutula JR, Raab H, Clark S, Bhakta S, Leipold DD, Weir S, et al. Site-specific conjugation of a cytotoxic drug to an antibody improves the therapeutic index. Nat Biotechnol 2008;26:925–32.
17. Austin CD, De Mazière AM, Pisacane PI, van Dijk SM, Eigenbrot C, Sliwkowski MX, et al. Endocytosis and sorting of ErbB2 and the site of action of cancer therapeutics trastuzumab and geldanamycin. Mol Biol Cell 2004;15:5268–82.
18. Doronina SO, Mendelsohn BA, Bovee TD, Cerveny CG, Alley SC, Meyer DL, et al. Enhanced activity of monomethylauristatin F through monoclonal antibody delivery: Effects of linker technology on efficacy and toxicity. Bioconjugate Chem 2006;17:114–24.
19. Kung Sutherland MS, Walter RB, Jeffrey SC, Burke PJ, Yu C, Kostner H, et al. SGN-CD33A: a novel CD33-targeting antibody-drug conjugate using a pyrrolobenzodiazepine dimer is active in models of drug-resistant AML. Blood 2013;122:1455–63.
20. Jeffrey SC, Burke PJ, Lyon RP, Meyer DW, Sussman D, Anderson M, et al. A potent anti-CD70 antibody-drug conjugate combining a dimeric pyrrolobenzodiazepine drug with site-specific conjugation technology. Bioconjugate Chem 2013;24:1256–63.
21. Saunders LR, Bankovich AJ, Anderson WC, Aujay MA, Bheddah S, Black K, et al. A DLL3-targeted antibody-drug conjugate eradicates high-grade pulmonary neuroendocrine tumor-initiating cells in vivo. Sci Transl Med 2015;7:302ra136–6.
22. Miller ML, Fishkin NE, Li W, Whiteman KR, Kovtun Y, Reid EE, et al. A new class of antibody-drug conjugates with potent DNA alkylating activity. Mol Cancer Ther 2016;15:1870–8.
23. Rudin CM, Pietanza MC, Bauer TM, Ready N, Morgensztern D, Glisson BS, et al. Rovalpituzumab tesirine, a DLL3-targeted antibody-drug conjugate, in recurrent small-cell lung cancer: a first-in-human, first-in-class, open-label, phase 1 study. Lancet Oncol 2017;18:42–51.
24. Zhang D, Pillow TH, Ma Y, Cruz-Chuh JD, Kozak KR, Sadowsky JD, et al. Linker immolation determines cell killing activity of disulfide-linked pyrrolobenzodiazepine antibody-drug conjugates. ACS Med Chem Lett 2016;7:988–93.
25. Montaser M, Lalmanach G, Mach L. CA-074, but not its methyl ester CA-074Me, is a selective inhibitor of cathepsin B within living cells. Biol Chem 2002;383:1305–8.
26. Choe Y, Leonetti F, Greenbaum DC, Lecaille F, Bogyo M, Brömme D, et al. Substrate profiling of cysteine proteases using a combinatorial peptide library identifies functionally unique specificities. J Biol Chem 2006;281:12824–32.
27. Allan ERO, Yates RM. Redundancy between cysteine cathepsins in murine experimental autoimmune encephalomyelitis. PLoS One 2015;10:e0128945.
28. Vasiljeva O, Papazoglou A, Krüger A, Brodoefel H, Korovin M, Deussing J, et al. Tumor cell-derived and macrophage-derived cathepsin B promotes progression and lung metastasis of mammary cancer. Cancer Res 2006;66:5242–50.
29. Sevenich L, Schurigt U, Sachse K, Gajda M, Werner F, Müller S, et al. Synergistic antitumor effects of combined cathepsin B and cathepsin Z deficiencies on breast cancer progression and metastasis in mice. Proc Natl Acad Sci U S A 2010;107:2497–502.
30. Dorywalska M, Dushin R, Moine L, Farias SE, Zhou D, Navaratnam T, et al. Molecular basis of valine-citrulline-PABC linker instability in site-specific ADCs and its mitigation by linker design. Mol Cancer Ther 2016;15:958–70.
31. Dal Corso A, Cazzamalli S, Gébleux R, Mattarella M, Neri D. Protease-cleavable linkers modulate the anticancer activity of non-internalizing antibody-drug conjugates. Bioconjugate Chem 2017;28:1826–33.
32. Roshy S, Sloane BF, Moin K. Pericellular cathepsin B and malignant progression. Cancer Metastasis Rev 2003;22:271–86.
33. Rodriguez-Franco EJ, Cantres-Rosario YM, Plaud-Valentin M, Romeu R, Rodríguez Y, Skolasky R, et al. Dysregulation of macrophage-secreted cathepsin B contributes to HIV-1-linked neuronal apoptosis. PLoS One 2012;7:e36571.
34. Sevenich L, Joyce JA. Pericellular proteolysis in cancer. Genes Dev 2014;28:2331–47.
35. Erickson HK, Park PU, Widdison WC, Kovtun YV, Garrett LM, Hoffman K, et al. Antibody-maytansinoid conjugates are activated in targeted cancer cells by lysosomal degradation and linker-dependent intracellular processing. Cancer Res 2006;66:4426–33.
36. Erickson HK, Lewis Phillips GD, Leipold DD, Provenzano CA, Mai E, Johnson HA, et al. The effect of different linkers on target cell catabolism and pharmacokinetics/pharmacodynamics of trastuzumab maytansinoid conjugates. Mol Cancer Ther 2012;11:1133–42.
37. Lehar SM, Pillow T, Xu M, Staben L, Kajihara KK, Vandlen R, et al. Novel antibody-antibiotic conjugate eliminates intracellular S. aureus. Nature 2015;527:323–8.
38. Mariathasan S, Tan M-W. Antibody–antibiotic conjugates: a novel therapeutic platform against bacterial infections. Trends Mol Med 2017;23:135–49.